Supplement of Atmos. Chem. Phys., 18, 11097–11124, 2018
https://doi.org/10.5194/acp-18-11097-2018-supplement

Atmospheric Chemistry and Physics
Open Access
EGU

Supplement of

A global synthesis inversion analysis of recent variability in CO_2 fluxes using GOSAT and in situ observations

James S. Wang et al.

Correspondence to: James S. Wang (james.s.wang@post.harvard.edu)

Table S1. In Situ Observation Sites Used in Inversions.

Site Code[a]	Name and Country	Latitude	Longitude	Elevation (m ASL)	Agency	Obs Type[b]	Mismatch (ppm)[c]	Mean Total Uncertainty (ppm)[d]
ABP	Arembepe, Bahia, Brazil	-12.77	-38.17	1	NOAA	F	1.25	2.50
ALT	Alert, Nunavut, Canada	82.45	-62.52	190	NOAA	F	0.75	1.51
AMT107	Argyle, Maine, U.S.	45.03	-68.68	53	NOAA	C	--	1.09
ASC	Ascension Island, UK	-7.97	-14.4	85	NOAA	F	0.4	0.82
ASK	Assekrem, Algeria	23.18	5.42	2710	NOAA	F	0.75	1.52
AZR	Terceira Island, Azores, Portugal	38.77	-27.38	19	NOAA	F	0.75	1.50
BAL	Baltic Sea, Poland	55.35	17.22	3	NOAA	F	4	8.03
BAO300	Boulder Atmospheric Observatory, Colorado, U.S.	40.05	-105	1584	NOAA	C	--	2.00
BKT	Bukit Kototabang, Indonesia	-0.2	100.32	845	NOAA	F	4	8.01
BMW	Tudor Hill, Bermuda, UK	32.27	-64.88	30	NOAA	F	0.75	1.53
BRW	Barrow, Alaska, U.S.	71.32	-156.6	11	NOAA	F	0.75	1.53
BSC	Black Sea, Constanta, Romania	44.17	28.67	0	NOAA	F	4	8.01
CBA	Cold Bay, Alaska, U.S.	55.2	-162.72	21	NOAA	F	0.75	1.51
CGO	Cape Grim, Tasmania, Australia	-40.68	144.69	94	NOAA	F	0.4	0.82
CHR	Christmas Island, Kiribati	1.7	-157.17	0	NOAA	F	0.4	0.82
CIB	Centro de Investigacion de la Baja Atmosfera, Spain	41.81	-4.93	845	NOAA	F	2.5	5.01
CPT	Cape Point, South Africa	-34.35	18.49	230	NOAA	F	0.75	1.51
CRZ	Crozet Island, France	-46.45	51.85	197	NOAA	F	0.4	0.82
DRP	Drake Passage	-59	-64.69	0	NOAA	F	0.4	0.83
DSI	Dongsha Island, Taiwan	20.7	116.73	3	NOAA	F	0.75	1.52
EIC	Easter Island, Chile	-27.15	-109.45	47	NOAA	F	0.75	1.53
GMI	Guam, Mariana Islands	13.43	144.78	0	NOAA	F	0.75	1.52
HBA	Halley Station, Antarctica, UK	-75.58	-26.21	30	NOAA	F	0.4	0.81
HPB	Hohenpeissenberg, Germany	47.8	11.01	936	NOAA	F	4	8.01
HSU	Humboldt State University, U.S.	41.06	-124.75	0	NOAA	F	0.75	1.52
HUN	Hegyhatsal, Hungary	46.95	16.65	248	NOAA	F	4	8.00
ICE	Storhofdi, Vestmannaeyjar, Iceland	63.4	-20.29	118	NOAA	F	0.75	1.51

IZO	Izana, Tenerife, Canary Islands, Spain	28.3	-16.48	2373	NOAA	F	0.75	1.52
KEY	Key Biscayne, Florida, U.S.	25.67	-80.2	1	NOAA	F	1.25	2.51
KUM	Cape Kumukahi, Hawaii, U.S.	19.52	-154.82	3	NOAA	F	0.75	1.62
KZD	Sary Taukum, Kazakhstan	44.45	77.57	595	NOAA	F	1.25	2.52
KZM	Plateau Assy, Kazakhstan	43.25	77.88	2519	NOAA	F	1.25	2.52
LEF396	Park Falls, Wisconsin, U.S.	45.93	-90.27	472	NOAA	C	--	0.94
LLB	Lac La Biche, Alberta, Canada	54.95	-112.45	540	NOAA	F	1.5	3.02
LLN	Lulin, Taiwan	23.47	120.87	2862	NOAA	F	1.25	2.53
LMP	Lampedusa, Italy	35.52	12.62	45	NOAA	F	0.75	1.51
MEX	High Altitude Global Climate Observation Center, Mexico	18.98	-97.31	4464	NOAA	F	1.25	2.51
MHD	Mace Head, County Galway, Ireland	53.33	-9.9	5	NOAA	F	1.25	2.51
MID	Sand Island, Midway, U.S.	28.21	-177.38	11	NOAA	F	0.75	1.52
MKN	Mt. Kenya, Kenya	-0.05	37.3	3644	NOAA	F	1.25	2.52
MLO	Mauna Loa, Hawaii, U.S.	19.54	-155.58	3397	NOAA	F	0.75	1.52
MNM	Minamitorishima, Japan	24.3	153.97	8	JMA	C	--	0.30
NAT	Farol De Mae Luiza Lighthouse, Brazil	-5.51	-35.26	50	NOAA	F	0.75	1.51
NMB	Gobabeb, Namibia	-23.58	15.03	456	NOAA	F	1.25	2.51
NWR	Niwot Ridge, Colorado, U.S.	40.05	-105.58	3523	NOAA	F	0.75	1.52
OXK	Ochsenkopf, Germany	50.07	11.8	1022	NOAA	F	1.25	2.52
PAL	Pallas-Sammaltunturi, GAW Station, Finland	67.97	24.12	565	NOAA	F	1.25	2.51
POCN00	Pacific Ocean (0 N)	0	-163	10	NOAA	F	0.4	0.82
POCN05	Pacific Ocean (5 N)	5	-158	10	NOAA	F	0.4	0.82
POCN10	Pacific Ocean (10 N)	10	-152	10	NOAA	F	0.4	0.85
POCN15	Pacific Ocean (15 N)	15	-147	10	NOAA	F	0.4	0.82
POCN20	Pacific Ocean (20 N)	20	-140	10	NOAA	F	0.4	0.84
POCN25	Pacific Ocean (25 N)	25	-134	10	NOAA	F	0.4	0.83
POCN30	Pacific Ocean (30 N)	30	-126	10	NOAA	F	0.4	0.83
POCS05	Pacific Ocean (5 S)	-5	-168	10	NOAA	F	0.4	0.82
POCS10	Pacific Ocean (10 S)	-10	-174	10	NOAA	F	0.4	0.80
POCS15	Pacific Ocean (15 S)	-15	-178	10	NOAA	F	0.4	0.82
POCS20	Pacific Ocean (20 S)	-20	-178.5	10	NOAA	F	0.4	0.84
POCS25	Pacific Ocean (25 S)	-25	174	10	NOAA	F	0.4	0.82

POCS30	Pacific Ocean (30 S)	-30	169	10	NOAA	F	0.4	0.85
PSA	Palmer Station, Antarctica, U.S.	-64.92	-64	10	NOAA	F	0.4	0.82
PTA	Point Arena, California, U.S.	38.95	-126.23	17	NOAA	F	2.5	5.01
RPB	Ragged Point, Barbados	13.17	-59.43	15	NOAA	F	0.75	1.51
RYO	Ryori, Japan	39.03	141.83	260	JMA	C	--	2.45
SCT305	Beech Island, South Carolina, U.S.	33.41	-81.83	115	NOAA	C	--	1.51
SDZ	Shangdianzi, China	40.65	117.12	293	NOAA	F	4	8.00
SEY	Mahe Island, Seychelles	-4.67	55.17	2	NOAA	F	0.4	0.82
SGP	Southern Great Plains, Oklahoma, U.S.	36.8	-97.5	314	NOAA	F	1.25	2.52
SHM	Shemya Island, Alaska, U.S.	52.72	174.1	23	NOAA	F	1.25	2.51
SMO	Tutuila, American Samoa	-14.24	-170.57	42	NOAA	F	0.4	0.81
SPO	South Pole, Antarctica, U.S.	-89.98	-24.8	2810	NOAA	F	0.4	0.81
STM	Ocean Station M, Norway	66	2	0	NOAA	F	0.75	1.50
SUM	Summit, Greenland	72.58	-38.48	3210	NOAA	F	0.75	1.51
SYO	Syowa Station, Antarctica, Japan	-69.01	39.58	14	NOAA	F	0.4	0.81
TAP	Tae-ahn Peninsula, Republic of Korea	36.73	126.13	16	NOAA	F	4	8.16
TDF	Tierra del Fuego, Argentina	-54.87	-68.48	20	NOAA	F	0.4	0.83
THD	Trinidad Head, California, U.S.	41.05	-124.15	107	NOAA	F	1.25	2.52
UTA	Wendover, Utah, U.S.	39.9	-113.72	1327	NOAA	F	1.25	2.52
UUM	Ulaan Uul, Mongolia	44.45	111.1	1007	NOAA	F	1.25	2.59
WBI379	West Branch, Iowa, U.S.	41.72	-91.35	242	NOAA	C	--	1.82
WGC483	Walnut Grove, California, U.S.	38.27	-121.49	0	NOAA	C	--	2.35
WIS	Weizmann Institute of Science at the Arava Institute, Ketura, Israel	31.13	34.88	151	NOAA	F	1.25	2.51
WKT457	Moody, Texas, U.S.	31.32	-97.33	251	NOAA	C	--	1.05
WLG	Mt. Waliguan, China	36.29	100.9	3810	NOAA	F	1.25	2.54
YON	Yonagunijima, Japan	24.47	123.02	30	JMA	C	--	1.08
ZEP	Ny-Alesund, Svalbard, Norway and Sweden	78.91	11.88	474	NOAA	F	0.75	1.52

[a] Tower intake height appended where relevant

[b] F = Flask, C = Continuous

[c] Model-data mismatch component of observation error

[d] Includes factor of 2 overall increase

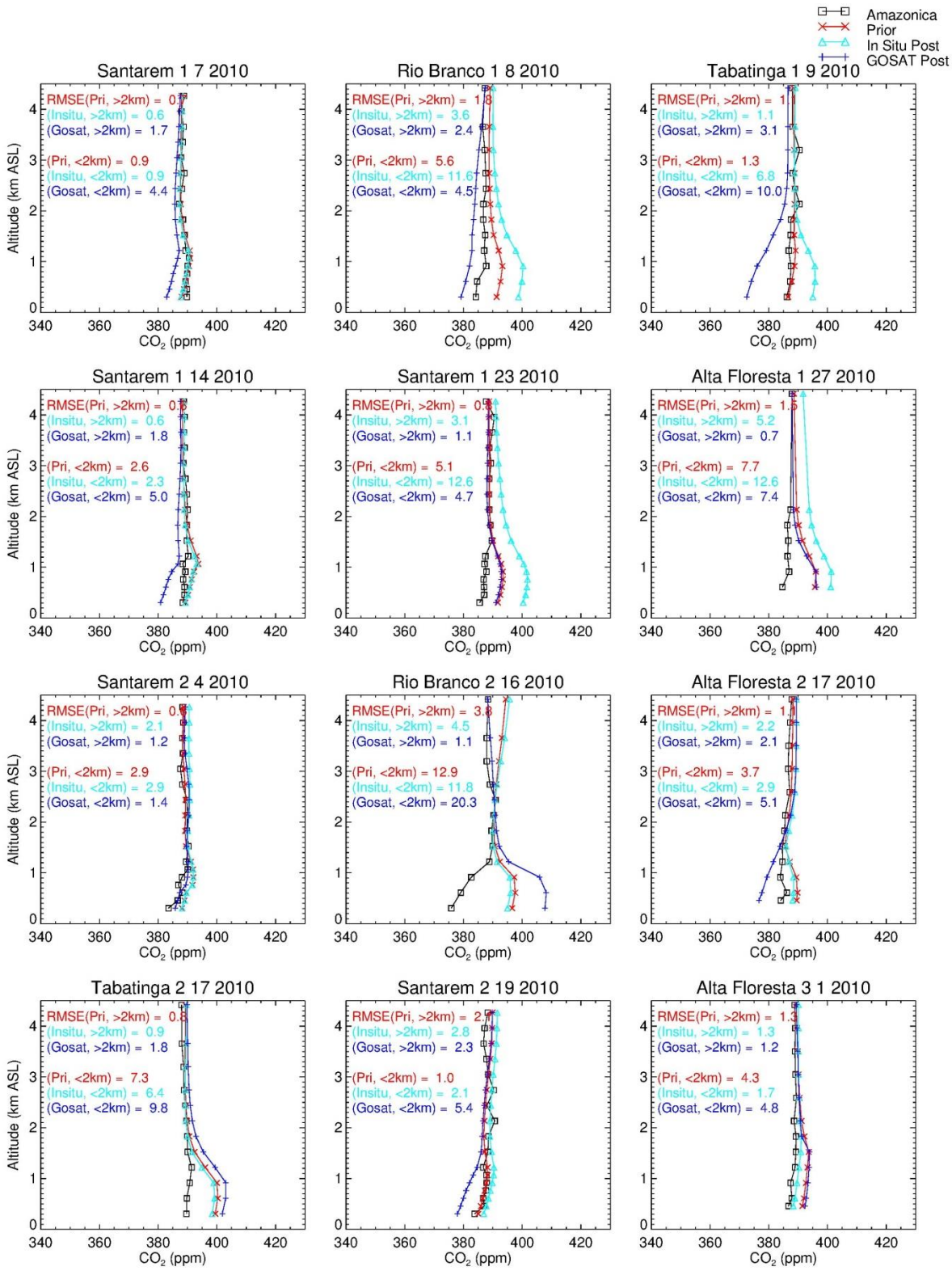

Figure S1. Comparison of prior, in situ-only posterior, GOSAT-only posterior, and Amazonica aircraft vertical profiles over 4 sites on different dates.

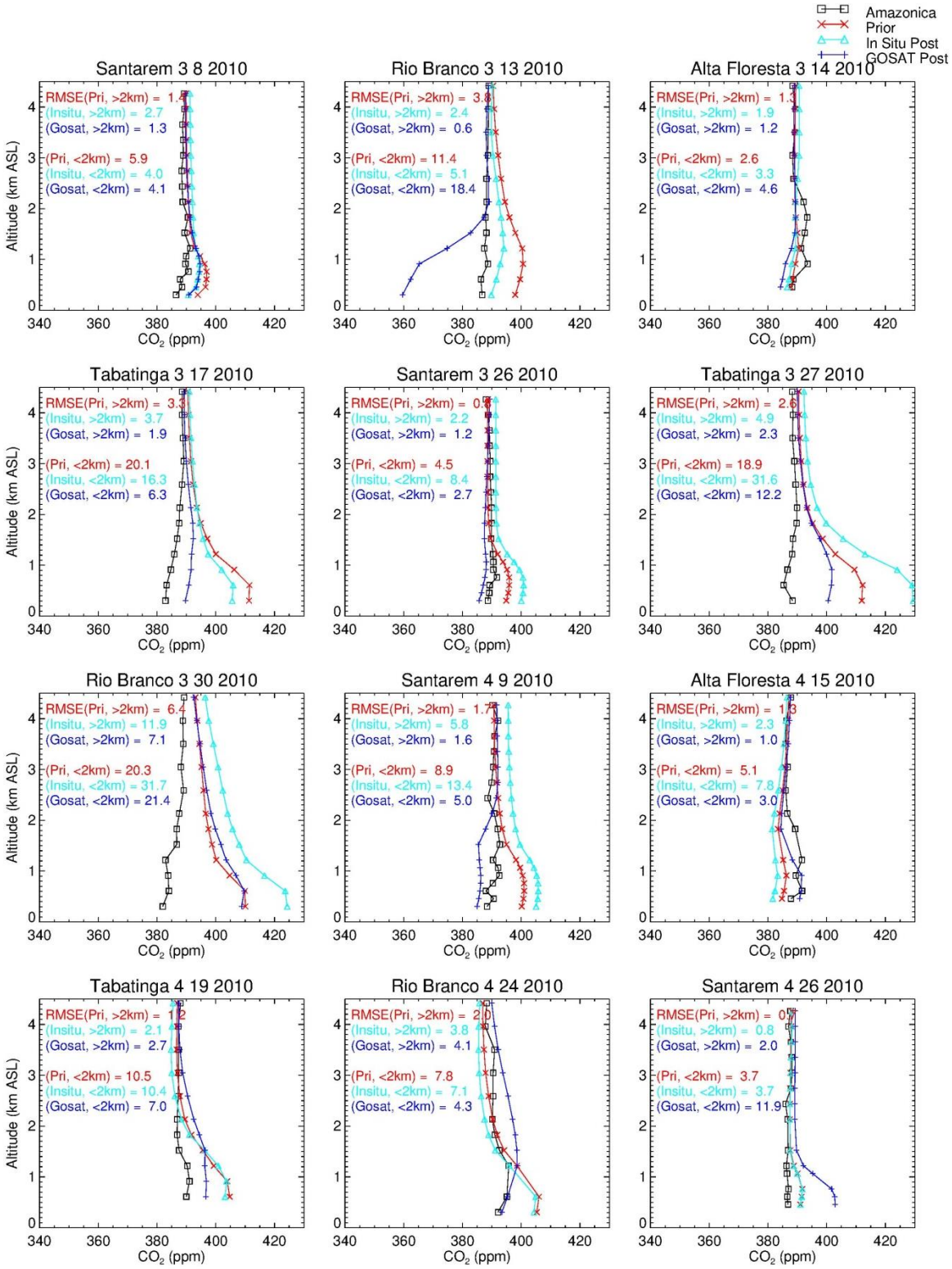

Figure S1. (continued)

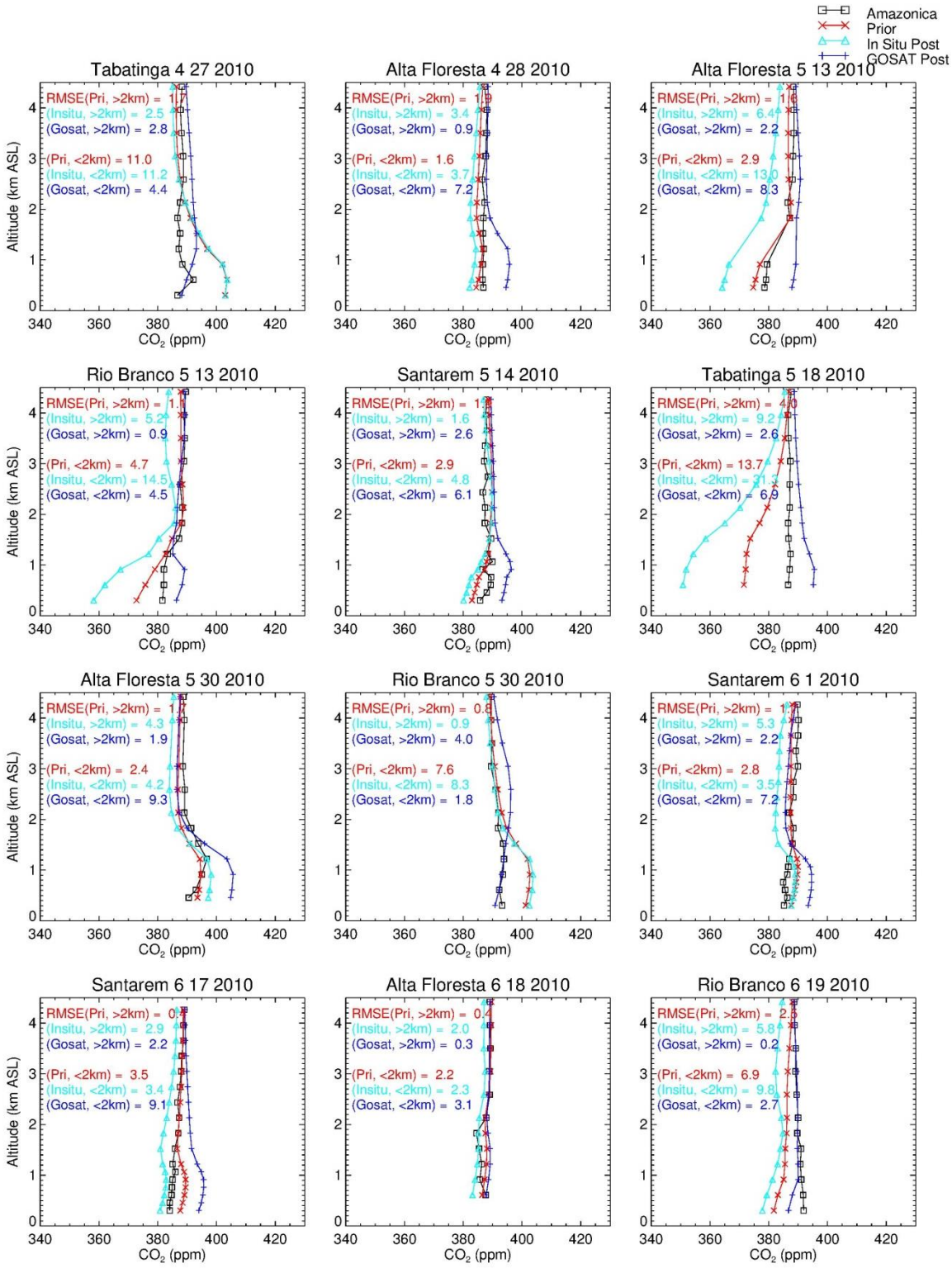

Figure S1. (continued)

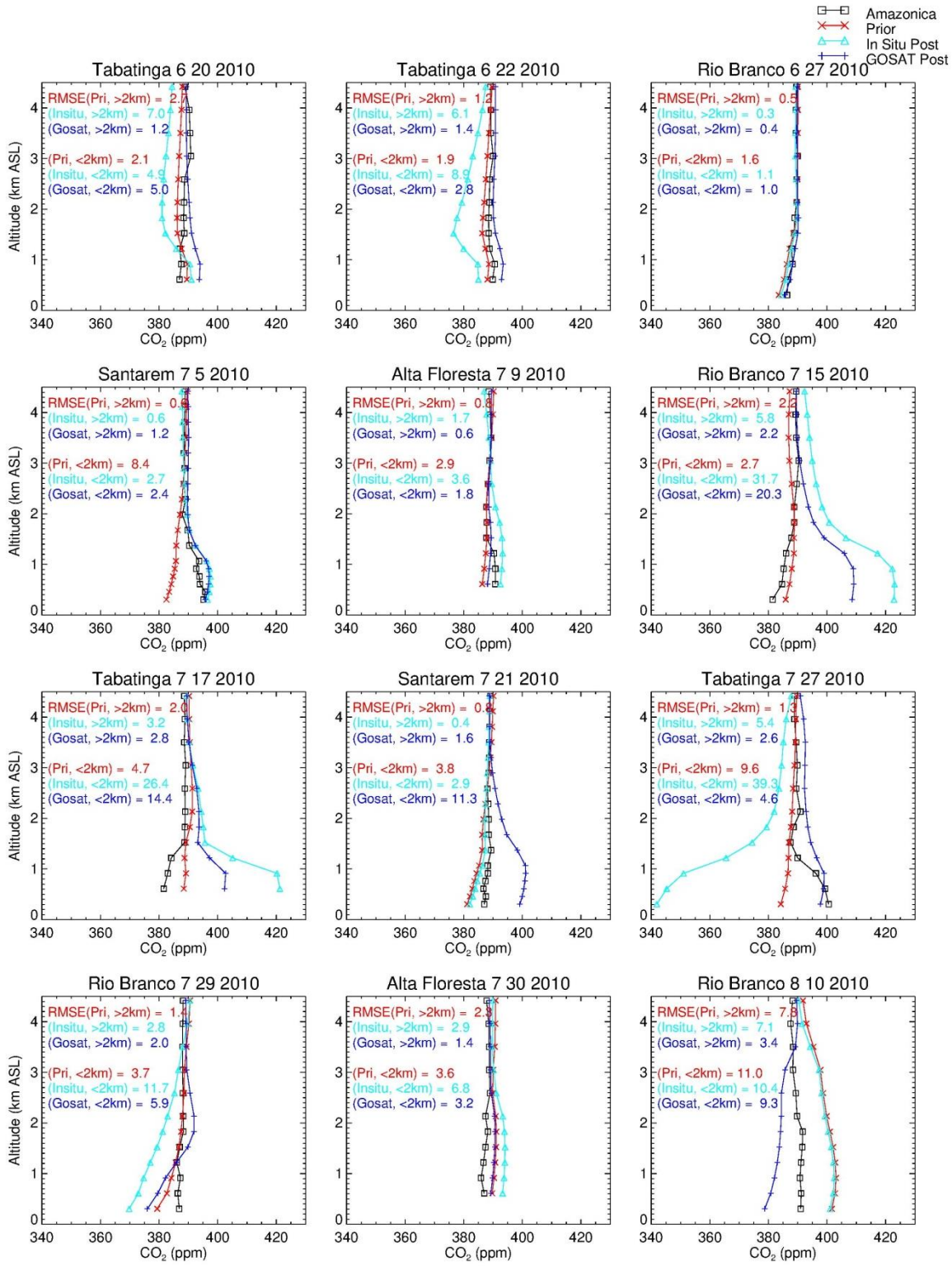

Figure S1. (continued)

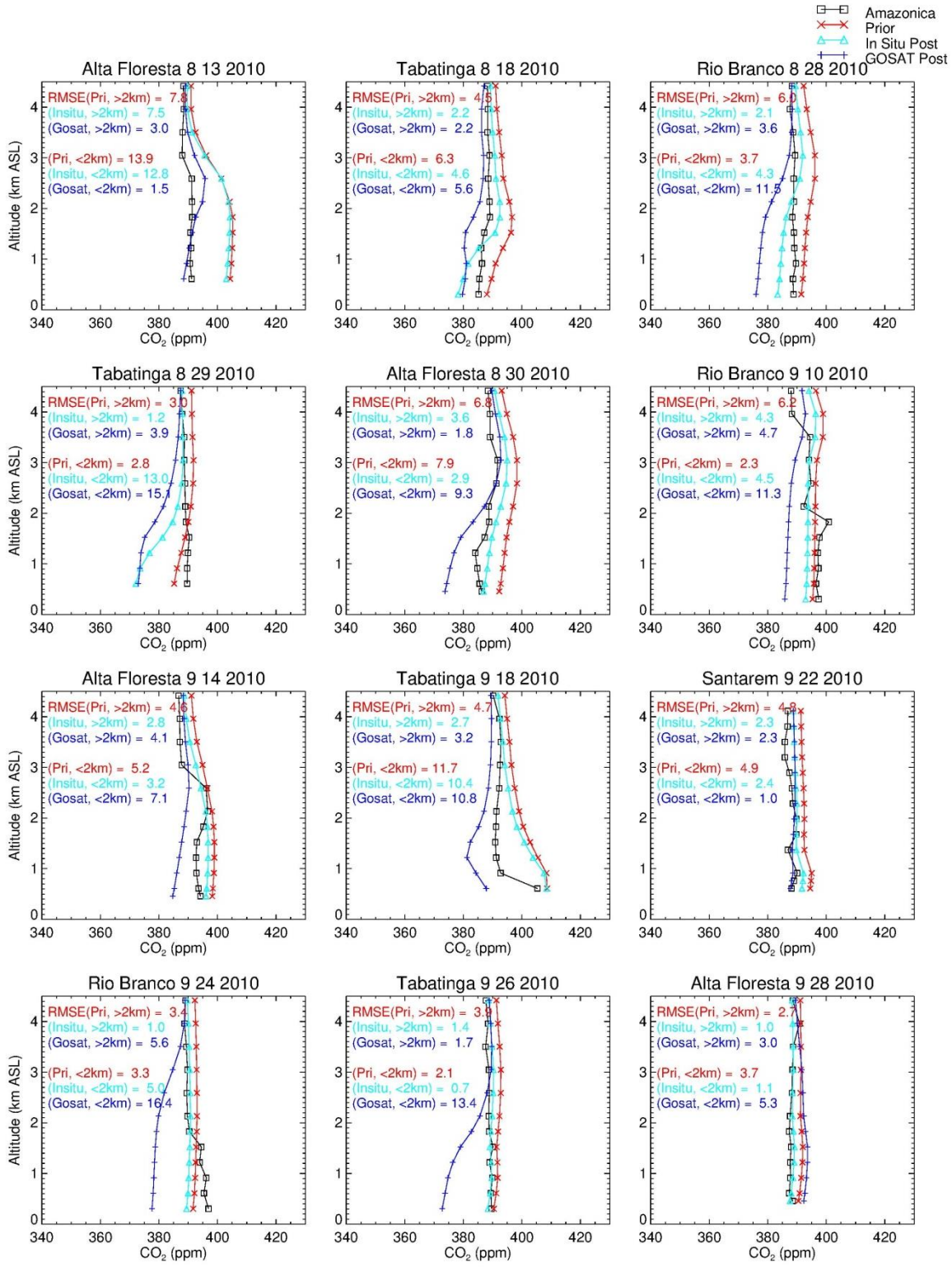

Figure S1. (continued)

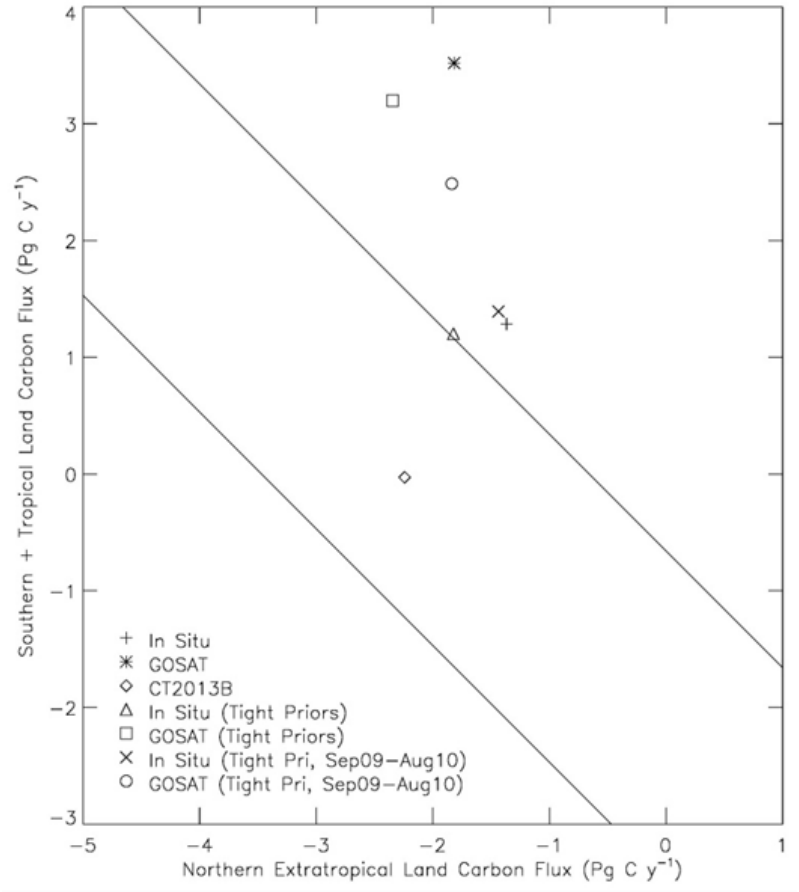

Figure S2. Posterior north-south land flux partitioning after Schimel et al. (2015). The diagonal lines are based on the global land carbon exchange (= land-use change emissions – land sink) estimated by GCP (2015) for the years relevant to the present analysis, i.e. 2009 and 2010, ± 1σ. Fluxes are for June 2009-May 2010 except where specified in the legend (for September 2009-August 2010). CT2013B refers to the CarbonTracker data assimilation system.

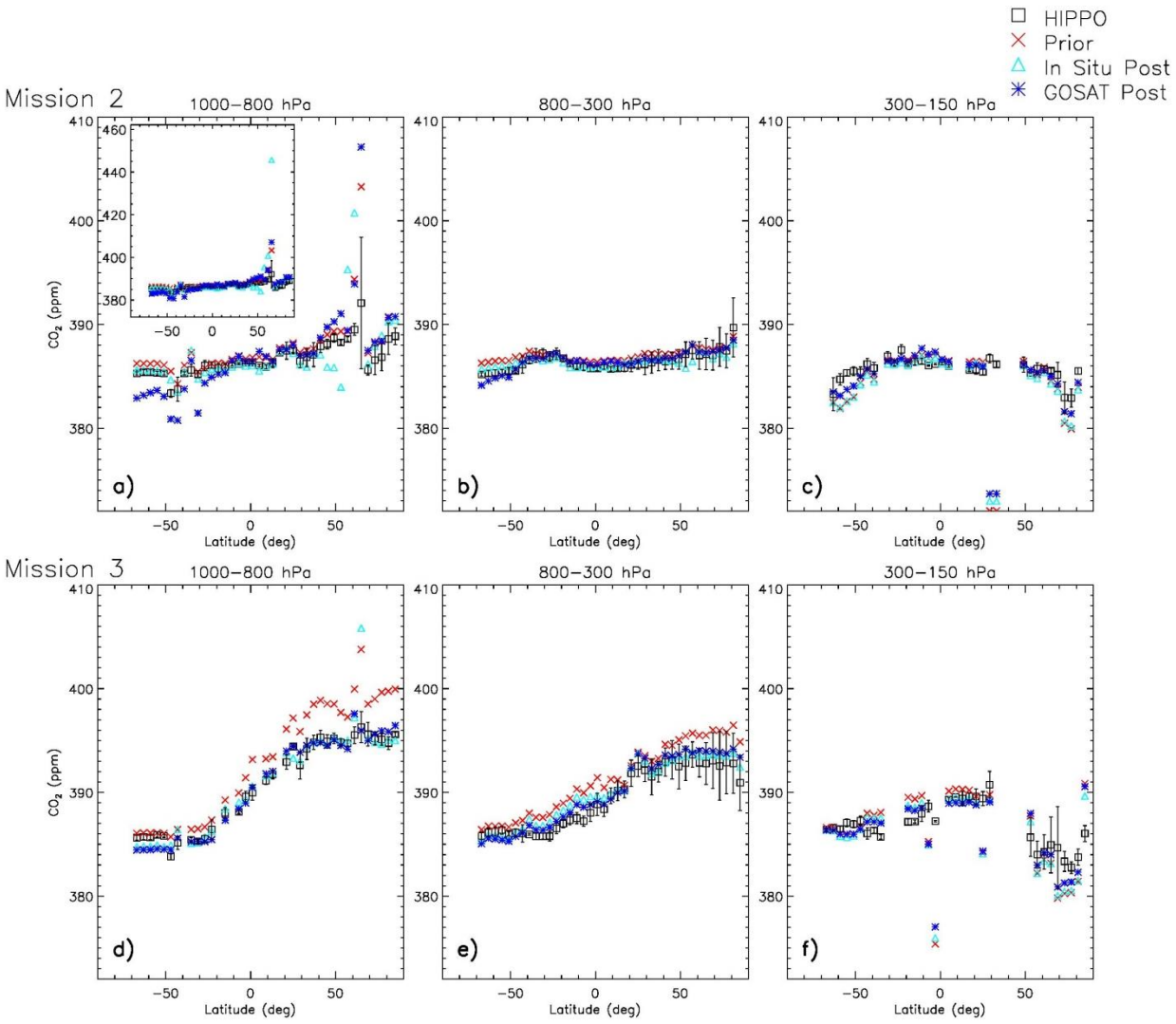

Figure S3. Same as Fig. 10 except showing inversions with tighter prior uncertainties.

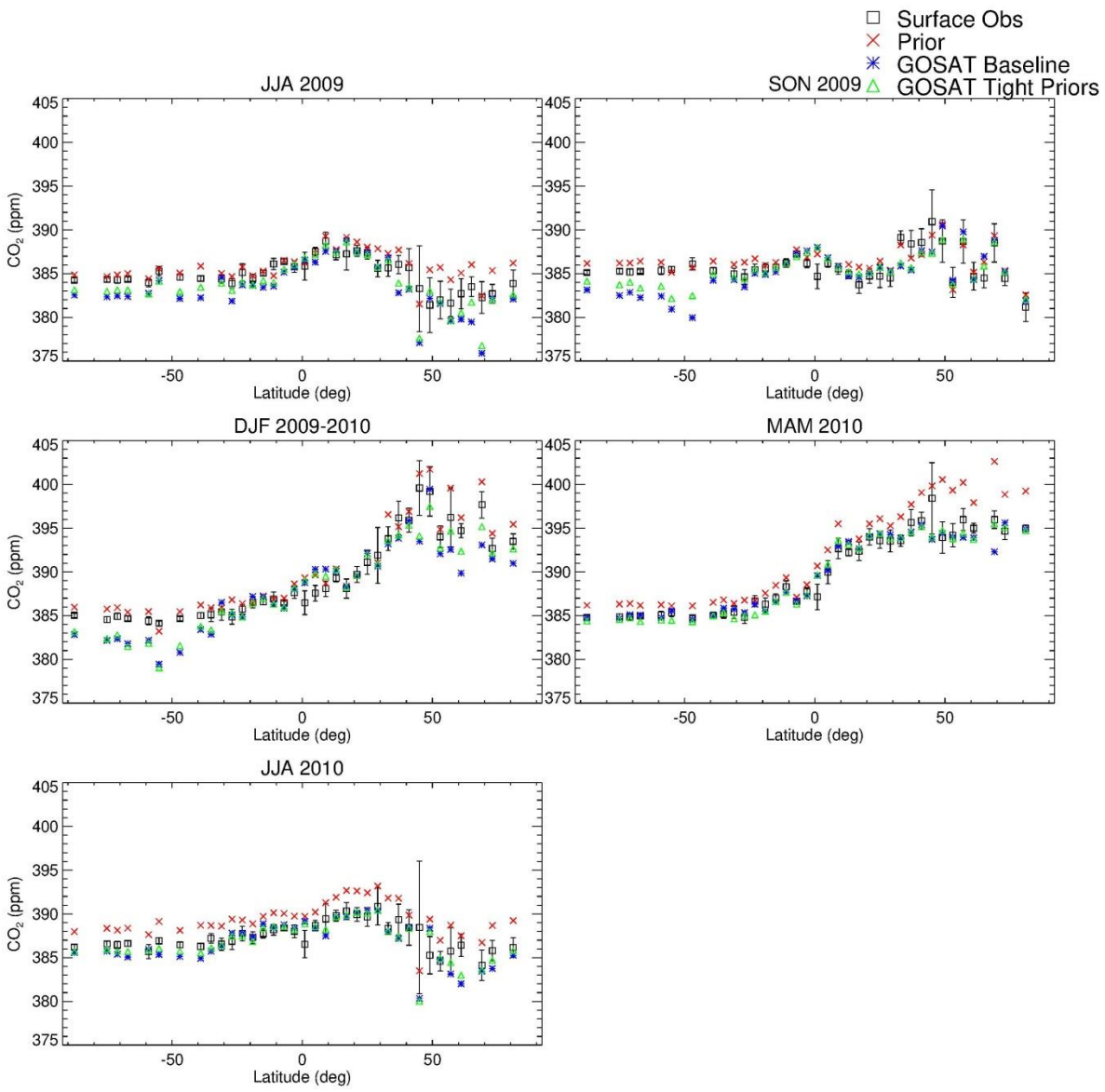

Figure S4. Same as Fig. 9 except showing GOSAT-only inversions with baseline vs. tighter prior uncertainties.